

Phase structure of (3+1)-dimensional dense two-color QCD at $T = 0$ in the strong coupling limit with tensor renormalization group

Yuto Sugimoto  ^a **Shinichiro Akiyama**  ^{b,c} **Yoshinobu Kuramashi**  ^b

^a *Department of Physics, Tohoku University, Sendai 980-8578, Japan*

^b *Center for Computational Sciences, University of Tsukuba, Tsukuba, Ibaraki 305-8577, Japan*

^c *Graduate School of Science, The University of Tokyo, Bunkyo-ku, Tokyo, 113-0033, Japan*

E-mail: sugimoto@nucl.phys.tohoku.ac.jp, akiyama@ccs.tsukuba.ac.jp,
kuramasi@het.ph.tsukuba.ac.jp

ABSTRACT: We investigate the phase structure of the (3+1)-dimensional strong coupling two-color QCD at zero temperature with finite chemical potential using the tensor renormalization group method. The chiral and diquark condensates and the quark number density are evaluated as a function of the chemical potential. Our results are compared with the previous analytical results using the mean field approximation. The critical exponents associated with the diquark condensation are also discussed.

Contents

1	Introduction	1
2	Formulation and numerical algorithm	2
2.1	Strong coupling QC ₂ D	2
2.2	Grassman tensor network representation	3
3	Numerical results	5
3.1	Chiral condensate and number density	5
3.2	Diquark condensate	6
4	Summary and outlook	8
A	Explicit form of F and R	9

1 Introduction

The complex action problem with finite chemical potential μ does not allow the standard Monte Carlo simulation to investigate the phase structure of QCD in the finite baryon density. On the other hand, the simulation of two-color QCD (QC₂D) with $\mu \neq 0$ is free from the complex action problem, so that it provides us an opportunity to understand the physics of matter under the finite density condition. Furthermore, in the strong coupling limit, we can use analytical methods to investigate the phase structure. In the 1980s, there were several mean field (MF) studies on chiral and diquark condensates in the strong coupling limit of the finite density QC₂D with staggered quarks [1–3]. The results were later refined by Nishida, including the QCD case [4, 5].

The tensor renormalization group (TRG) method¹ may be qualified to investigate the phase structure of finite density QCD: This method, which is in principle free from the sign problem or the complex action problem, has been successfully applied to various types of models with these problems [8, 15, 18–37]. As a preparatory study before exploring (3+1)-dimensional ((3+1) d) finite density QCD, it would be a good idea to apply the TRG method to the strong coupling limit of (3+1) d finite density QC₂D, which becomes much simpler with vanishing gauge action. Firstly, we already have some insight into the phase structure thanks to a recent study of (1+1) d finite density QC₂D with the TRG method, including the finite coupling case [38]. Secondly, it is useful to compare the TRG results with the MF ones [4]. Especially, the TRG method is allowed to investigate the phase structure at zero temperature, where the standard Monte Carlo approach is hardly

¹In this paper, the “TRG method” or the “TRG approach” refers to not only the original numerical algorithm proposed by Levin and Nave [6] but also its extensions [7–17].

accessible. Thirdly, the computational techniques employed in our previous study on the (3+1) d finite density Nambu–Jona-Lasinio model [15] are readily applicable to the strong coupling case.

In this paper, we investigate the phase structure of the strong coupling limit of the finite density QC₂D with the staggered quark, measuring the chiral and diquark condensates and the quark number density as a function of μ . Our results are compared with the analytical results obtained by the MF method and the $1/d_s$ expansion with d_s the spatial dimension [4].

This paper is organized as follows. In Sec. 2, we define the action of the QC₂D with finite chemical potential and give the tensor network representation. In Sec. 3 we measure the chiral and diquark condensates and the quark number density as a function of the chemical potential. The critical exponents are also determined. The results are compared with the analytical ones in Ref. [4]. Section 4 is devoted to summary and outlook.

2 Formulation and numerical algorithm

2.1 Strong coupling QC₂D

We consider the finite density QC₂D on a (3+1) d lattice $\Lambda_{3+1} = \{(n_1, n_2, n_3, n_4) | n_{1,2,3} = 1, \dots, N_s, n_4 = 1, \dots, N_\tau\}$ whose volume is $V = N_s^3 \times N_\tau$. The lattice spacing a is set to $a = 1$ unless necessary. The action consists of the gluonic part and the fermionic one. For the former, the simple plaquette action is given by

$$S_G = \frac{2N_c}{g^2} \sum_{n,\nu,\rho} \left\{ 1 - \frac{1}{N_c} \text{ReTr} \left(U_\nu(n) U_\rho(n + \hat{\nu}) U_\nu^\dagger(n + \hat{\rho}) U_\rho^\dagger(n) \right) \right\} \quad (2.1)$$

with $N_c = 2$ and g the gauge coupling constant. The SU(N_c)-valued link variable between the sites n and $n + \hat{\nu}$, with $\hat{\nu}$ the unit vector in the ν direction, is denoted by $U_\nu(n)$. For the latter we employ the Kogut-Susskind quark action with the finite chemical potential μ :

$$S_F = \sum_n \left[\frac{1}{2} \sum_\nu \eta_\nu(n) \left\{ e^{i\mu\delta_{\nu,4}} \bar{\chi}(n) U_\nu(n) \chi(n + \hat{\nu}) - e^{-i\mu\delta_{\nu,4}} \bar{\chi}(n + \hat{\nu}) U_\nu^\dagger(n) \chi(n) \right\} + m \bar{\chi}(n) \chi(n) \right] \quad (2.2)$$

with m the quark mass. $\chi = (\chi^1, \chi^2, \dots, \chi^{N_c})$ is a N_c component Grassmann variables, and $\eta_\nu(n)$ is the staggered sign function defined by $\eta_\nu(n) = (-1)^{n_1 + \dots + n_{\nu-1}}$ with $\eta_1(n) = 1$. Note that Eq. (2.2) is invariant under the following continuous chiral transformation at $m = \mu = 0$:

$$\chi(n) \rightarrow e^{i\alpha\epsilon(n)} \chi(n), \quad (2.3)$$

$$\bar{\chi}(n) \rightarrow \bar{\chi}(n) e^{i\alpha\epsilon(n)} \quad (2.4)$$

with $\alpha \in \mathbb{R}$ and $\epsilon(n) = (-1)^{n_1 + n_2 + n_3 + n_4}$.

The partition function is defined as

$$Z = \int \left(\prod_{n \in \Lambda_{3+1}, \nu} d\chi(n) d\bar{\chi}(n) dU_\nu(n) \right) e^{-S_G - S_F - S_D}, \quad (2.5)$$

where S_D is a source term to detect the diquark condensate given by

$$S_D = \frac{\lambda}{2} \{ \chi^t \tau_2 \chi + \bar{\chi} \tau_2 \bar{\chi}^t \} \quad (2.6)$$

with τ_2 the second Pauli matrix acting on the color space. In the strong coupling limit $g \rightarrow \infty$, the gluonic action vanishes because of the overall factor of $1/g^2$, and the link variables are left only in the fermionic action.

2.2 Grassmann tensor network representation

In order to apply tensor network methods to this system, it is necessary to rewrite the partition function Z in Eq. (2.5) as a product of local tensors. Since the theory involves fermionic degrees of freedom, we must properly incorporate their anticommuting nature. To this end, we employ a Grassmann tensor network formulation [39], in which the local tensors are defined using auxiliary Grassmann variables.

For clarity, let us consider the case $\lambda = 0$, which simplifies the discussion. The extension to $\lambda \neq 0$ is straightforward. To obtain the Grassmann tensor network representation of the partition function in Eq. (2.5), We introduce two-component auxiliary Grassmann variables ζ_ν and ξ_ν ($\nu = 1, 2, 3, 4$) [39]. As a basic tool, for any N -component Grassmann variable θ_i , one can use the identity

$$\int_{\bar{\theta}, \theta} := \int \prod_{i=1}^N d\bar{\theta}_i d\theta_i e^{\theta_i \bar{\theta}_i} = 1. \quad (2.7)$$

By inserting Eq. (2.7) into the hopping terms of S_F for each of the auxiliary variables ζ_ν and ξ_ν ,

$$\begin{aligned} & \exp \left[-\frac{\eta_\nu(n)}{2} e^{\mu \delta_{\nu,4}} \bar{\chi}(n) U_\nu(n) \chi(n + \hat{\nu}) \right] \\ &= \iint_{\zeta_\nu(n), \zeta_\nu(n)} \exp \left[-\frac{\eta_\nu(n)}{2} e^{\mu \delta_{\nu,4}} \bar{\chi}(n) \zeta_\nu(n) + \bar{\zeta}_\nu(n) U_\nu(n) \chi(n + \hat{\nu}) \right] \end{aligned} \quad (2.8)$$

$$\begin{aligned} & \exp \left[\frac{\eta_\nu(n)}{2} e^{-\mu \delta_{\nu,4}} \bar{\chi}(n + \hat{\nu}) U_\nu^\dagger(n) \chi(n) \right] \\ &= \iint_{\xi_\nu(n), \xi_\nu(n)} \exp \left[\bar{\chi}(n + \hat{\nu}) U_\nu^\dagger(n) \bar{\xi}_\nu(n) - \frac{\eta_\nu(n)}{2} e^{-\mu \delta_{\nu,4}} \xi_\nu(n) \chi(n) \right], \end{aligned} \quad (2.9)$$

we can define the local Grassmann tensor \mathcal{T} by integrating out link variables $U_\nu(n)$ and the staggered fields $\chi(n), \bar{\chi}(n)$ at each lattice site n ,

$$\begin{aligned} \mathcal{T} = \int \left[\prod_\nu dU_\nu \right] d\chi d\bar{\chi} e^{-m \bar{\chi} \chi} \prod_\nu & \left\{ \exp \left[-\frac{\eta_\nu(n)}{2} e^{\mu \delta_{\nu,4}} \bar{\chi} \zeta_\nu(n) + \bar{\zeta}_\nu(n - \hat{\nu}) U_\nu(n - \hat{\nu}) \chi \right] \right. \\ & \times \left. \exp \left[\bar{\chi} U_\nu^\dagger(n - \hat{\nu}) \bar{\xi}_\nu(n - \hat{\nu}) - \frac{\eta_\nu(n)}{2} e^{-\mu \delta_{\nu,4}} \xi_\nu(n) \chi \right] \right\}. \end{aligned} \quad (2.10)$$

$$\begin{aligned}
&= \sum_{\{i,j\}} \int \left[\prod_{\nu} dU_{\nu} \right] d\chi^1 d\bar{\chi}^1 d\chi^2 d\bar{\chi}^2 e^{-m\bar{\chi}\chi} \left[\prod_{\nu} \left(-\frac{\eta_{\nu}(n)}{2} e^{\mu\delta_{\nu,4}} \right)^{i_{\nu}^1+i_{\nu}^2} \left(-\frac{\eta_{\nu}(n)}{2} e^{-\mu\delta_{\nu,4}} \right)^{j_{\nu}^1+j_{\nu}^2} \right] \\
&\quad \times \left[\prod_{\nu} \left(\sum_{a_{\nu}} \bar{\zeta}_{\nu}^2 U_{\nu}^{2a_{\nu}} \chi^{a_{\nu}} \right)^{i_{\nu}^{\prime 2}} \right] \left[\prod_{\nu} \left(\sum_{b_{\nu}} \bar{\zeta}_{\nu}^1 U_{\nu}^{1b_{\nu}} \chi^{b_{\nu}} \right)^{i_{\nu}^{\prime 1}} \right] \left[\prod_{\nu} (\xi_{\nu}^1 \chi^1)^{j_{\nu}^1} \right] \left[\prod_{\nu} (\xi_{\nu}^2 \chi^2)^{j_{\nu}^2} \right] \\
&\quad \times \left[\prod_{\nu} \left(\sum_{c_{\nu}} \bar{\chi}^{c_{\nu}} U_{\nu}^{c_{\nu}2\dagger} \bar{\xi}_{\nu}^2 \right)^{j_{\nu}^{\prime 2}} \right] \left[\prod_{\nu} \left(\sum_{d_{\nu}} \bar{\chi}^{d_{\nu}} U_{\nu}^{d_{\nu}1\dagger} \bar{\xi}_{\nu}^1 \right)^{j_{\nu}^{\prime 1}} \right] \left[\prod_{\nu} (\bar{\chi}^1 \zeta_{\nu}^1)^{i_{\nu}^1} \right] \left[\prod_{\nu} (\bar{\chi}^2 \zeta_{\nu}^2)^{i_{\nu}^2} \right]. \tag{2.11}
\end{aligned}$$

In the above, we have introduced the fermion occupation numbers $i_{\nu}^1, i_{\nu}^2, j_{\nu}^1, j_{\nu}^2, j_{\nu}^{\prime 1}, j_{\nu}^{\prime 2}, i_{\nu}^1, i_{\nu}^2 \in \{0, 1\}$ ($\nu = 1, 2, 3, 4$), which arise from the Taylor expansion of Eq. (2.10), and the auxiliary integer variables $a_{\nu}, b_{\nu}, c_{\nu}, d_{\nu} \in \{1, 2\}$ to sum out the color indices of the staggered fields χ connected to the link variables U_{ν} . The summation $\sum_{\{i,j\}}$ denotes $\left(\prod_{\nu} \sum_{i_{\nu}^1, i_{\nu}^2, j_{\nu}^1, j_{\nu}^2, j_{\nu}^{\prime 1}, j_{\nu}^{\prime 2}, i_{\nu}^1, i_{\nu}^2} \right)$. Here we omit the explicit spacetime dependence except for $\eta_{\nu}(n)$. This implies that there are eight types of initial tensors, depending on the staggered sign [15].

To carry out the group integral over U_{ν} in Eq. (2.11), we introduce the indicator function $g(i) = \frac{1}{2}\delta_{i,0} + \delta_{i,1}$. Using this function, the Grassmann variables and the link variables can be separated as follows:

$$\left(\sum_{a_{\nu}} \bar{\zeta}_{\nu}^2 U_{\nu}^{2a_{\nu}} \chi^{a_{\nu}} \right)^{i_{\nu}^{\prime 2}} = g(i_{\nu}^{\prime 2}) \sum_{a_{\nu}} \left[(\bar{\zeta}_{\nu}^2)^{i_{\nu}^{\prime 2}} (U_{\nu}^{2a_{\nu}})^{i_{\nu}^{\prime 2}} (\chi^{a_{\nu}})^{i_{\nu}^{\prime 2}} \right]. \tag{2.12}$$

Thus, within the sum of $\sum_{a_{\nu}, b_{\nu}, c_{\nu}, d_{\nu}}$, we can analytically integrate the link variables,

$$F_{i_{\nu}^{\prime 2} i_{\nu}^1 j_{\nu}^2 j_{\nu}^1}^{a_{\nu} b_{\nu} c_{\nu} d_{\nu}} = g(i_{\nu}^{\prime 2}) g(i_{\nu}^1) g(j_{\nu}^1) g(j_{\nu}^2) \int dU_{\nu} (U_{\nu}^{2a_{\nu}})^{i_{\nu}^{\prime 2}} (U_{\nu}^{1b_{\nu}})^{i_{\nu}^1} (U_{\nu}^{c_{\nu}2\dagger})^{j_{\nu}^{\prime 2}} (U_{\nu}^{d_{\nu}1\dagger})^{j_{\nu}^1}, \tag{2.13}$$

where $F_{i_{\nu}^{\prime 2} i_{\nu}^1 j_{\nu}^2 j_{\nu}^1}^{a_{\nu} b_{\nu} c_{\nu} d_{\nu}}$ indicates the results of the integration using Weingarten calculus [40]. After integrating out the gauge fields, all that remains is to integrate out χ and $\bar{\chi}$. A straightforward calculation yields the final form of the Grassmann tensor \mathcal{T} :

$$\begin{aligned}
&\mathcal{T}_{\Psi_1(n)\Psi_2(n)\Psi_3(n)\Psi_4(n)\bar{\Psi}_4(n-\hat{4})\bar{\Psi}_3(n-\hat{2})\bar{\Psi}_2(n-\hat{2})\bar{\Psi}_1(n-\hat{1})} \\
&= \sum_{i,j,i',j'} T_{(i_1^1, i_1^2, j_1^1, j_1^2)(i_2^1, i_2^2, j_2^1, j_2^2)(i_3^1, i_3^2, j_3^1, j_3^2)(i_4^1, i_4^2, j_4^1, j_4^2)(i_1'^1, i_1'^2, j_1'^1, j_1'^2)(i_2'^1, i_2'^2, j_2'^1, j_2'^2)(i_3'^1, i_3'^2, j_3'^1, j_3'^2)(i_4'^1, i_4'^2, j_4'^1, j_4'^2)} \\
&\quad \times \left[(\zeta_1^1)^{i_1^1} (\zeta_1^2)^{i_1^2} (\xi_1^1)^{j_1^1} (\xi_1^2)^{j_1^2} \right] \left[(\zeta_2^1)^{i_2^1} (\zeta_2^2)^{i_2^2} (\xi_2^1)^{j_2^1} (\xi_2^2)^{j_2^2} \right] \left[(\zeta_3^1)^{i_3^1} (\zeta_3^2)^{i_3^2} (\xi_3^1)^{j_3^1} (\xi_3^2)^{j_3^2} \right] \left[(\zeta_4^1)^{i_4^1} (\zeta_4^2)^{i_4^2} (\xi_4^1)^{j_4^1} (\xi_4^2)^{j_4^2} \right] \\
&\quad \times \left[(\bar{\xi}_4^2)^{j_4'^2} (\bar{\xi}_4^1)^{j_4'^1} (\bar{\zeta}_4^1)^{j_4'^1} (\bar{\zeta}_4^2)^{i_4'^1} \right] \left[(\bar{\xi}_3^2)^{j_3'^2} (\bar{\xi}_3^1)^{j_3'^1} (\bar{\zeta}_3^2)^{i_3'^1} (\bar{\zeta}_3^1)^{i_3'^1} \right] \left[(\bar{\xi}_2^2)^{j_2'^2} (\bar{\xi}_2^1)^{j_2'^1} (\bar{\zeta}_2^2)^{i_2'^2} (\bar{\zeta}_2^1)^{i_2'^1} \right] \left[(\bar{\xi}_1^2)^{j_1'^2} (\bar{\xi}_1^1)^{j_1'^1} (\bar{\zeta}_1^2)^{i_1'^2} (\bar{\zeta}_1^1)^{i_1'^1} \right], \tag{2.14}
\end{aligned}$$

where $\Psi_{\nu} = (\zeta_{\nu}^1, \zeta_{\nu}^2, \xi_{\nu}^1, \xi_{\nu}^2)$ and $\bar{\Psi}_{\nu} = (\bar{\zeta}_{\nu}^1, \bar{\zeta}_{\nu}^2, \bar{\xi}_{\nu}^1, \bar{\xi}_{\nu}^2)$ denote the composite Grassmann variables, and the coefficient tensor T is defined as

$$T_{(i_1^1, i_1^2, j_1^1, j_1^2)(i_2^1, i_2^2, j_2^1, j_2^2)(i_3^1, i_3^2, j_3^1, j_3^2)(i_4^1, i_4^2, j_4^1, j_4^2)(i_1'^1, i_1'^2, j_1'^1, j_1'^2)(i_2'^1, i_2'^2, j_2'^1, j_2'^2)(i_3'^1, i_3'^2, j_3'^1, j_3'^2)(i_4'^1, i_4'^2, j_4'^1, j_4'^2)} = \dots$$

$$\begin{aligned}
&= \sum_{i,j} \left[\prod_{\nu} \left(-\frac{\eta_{\nu}(n)}{2} e^{\mu \delta_{\nu,4}} \right)^{i_{\nu}^1 + i_{\nu}^2} \left(-\frac{\eta_{\nu}(n)}{2} e^{-\mu \delta_{\nu,4}} \right)^{j_{\nu}^1 + j_{\nu}^2} \right] \left(\prod_{\nu} \sum_{a_{\nu}, b_{\nu}, c_{\nu}, d_{\nu}} \right) \left(\prod_{\nu} \tilde{F}_{i_{\nu}^{\prime 2} i_{\nu}^{\prime 1} j_{\nu}^{\prime 2} j_{\nu}^{\prime 1}}^{a_{\nu} b_{\nu} c_{\nu} d_{\nu}} \right) \\
&\times \left(-\delta_{1, \sum_{\nu} (\delta^{1,a_{\nu}} i_{\nu}^{\prime 2} + \delta^{1,b_{\nu}} i_{\nu}^{\prime 1} + j_{\nu}^1)} \delta_{1, \sum_{\nu} (\delta^{2,a_{\nu}} i_{\nu}^{\prime 2} + \delta^{2,b_{\nu}} i_{\nu}^{\prime 1} + j_{\nu}^2)} \delta_{1, \sum_{\nu} (\delta^{1,c_{\nu}} j_{\nu}^{\prime 2} + \delta^{1,d_{\nu}} j_{\nu}^{\prime 1} + i_{\nu}^1)} \delta_{1, \sum_{\nu} (\delta^{2,c_{\nu}} j_{\nu}^{\prime 2} + \delta^{2,d_{\nu}} j_{\nu}^{\prime 1} + i_{\nu}^2)} \right. \\
&+ m \delta_{1, \sum_{\nu} (\delta^{1,a_{\nu}} i_{\nu}^{\prime 2} + \delta^{1,b_{\nu}} i_{\nu}^{\prime 1} + j_{\nu}^1)} \delta_{0, \sum_{\nu} (\delta^{2,a_{\nu}} i_{\nu}^{\prime 2} + \delta^{2,b_{\nu}} i_{\nu}^{\prime 1} + j_{\nu}^2)} \delta_{1, \sum_{\nu} (\delta^{1,c_{\nu}} j_{\nu}^{\prime 2} + \delta^{1,d_{\nu}} j_{\nu}^{\prime 1} + i_{\nu}^1)} \delta_{0, \sum_{\nu} (\delta^{2,c_{\nu}} j_{\nu}^{\prime 2} + \delta^{2,d_{\nu}} j_{\nu}^{\prime 1} + i_{\nu}^2)} \\
&+ m \delta_{0, \sum_{\nu} (\delta^{1,a_{\nu}} i_{\nu}^{\prime 2} + \delta^{1,b_{\nu}} i_{\nu}^{\prime 1} + j_{\nu}^1)} \delta_{1, \sum_{\nu} (\delta^{2,a_{\nu}} i_{\nu}^{\prime 2} + \delta^{2,b_{\nu}} i_{\nu}^{\prime 1} + j_{\nu}^2)} \delta_{0, \sum_{\nu} (\delta^{1,c_{\nu}} j_{\nu}^{\prime 2} + \delta^{1,d_{\nu}} j_{\nu}^{\prime 1} + i_{\nu}^1)} \delta_{1, \sum_{\nu} (\delta^{2,c_{\nu}} j_{\nu}^{\prime 2} + \delta^{2,d_{\nu}} j_{\nu}^{\prime 1} + i_{\nu}^2)} \\
&+ m^2 \delta_{0, \sum_{\nu} (i_{\nu}^{\prime 2} + i_{\nu}^{\prime 1} + j_{\nu}^1 + j_{\nu}^2 + j_{\nu}^{\prime 2} + j_{\nu}^{\prime 1} + i_{\nu}^1 + i_{\nu}^2)} \left. \right) \\
&(-1)^R(i_1^1, i_1^2, j_1^1, j_1^2)(i_2^1, i_2^2, j_2^1, j_2^2)(i_3^1, i_3^2, j_3^1, j_3^2)(i_4^1, i_4^2, j_4^1, j_4^2)(i_1^{\prime 1}, i_1^{\prime 2}, j_1^{\prime 1}, j_1^{\prime 2})(i_2^{\prime 1}, i_2^{\prime 2}, j_2^{\prime 1}, j_2^{\prime 2})(i_3^{\prime 1}, i_3^{\prime 2}, j_3^{\prime 1}, j_3^{\prime 2})(i_4^{\prime 1}, i_4^{\prime 2}, j_4^{\prime 1}, j_4^{\prime 2}). \tag{2.15}
\end{aligned}$$

The tensor \tilde{F} is a redefined version of F that incorporates a, b, c, d dependence of the sign factors arising from the reordering of $\chi^2, \chi^1, \bar{\chi}^2, \bar{\chi}^1$ in the integration procedure. The tensor R likewise includes sign factors originating from the rearrangement of the auxiliary Grassmann fields $\zeta, \xi, \bar{\zeta}, \bar{\xi}$ to the form of Eq. (2.14). The explicit definitions of F , \tilde{F} , and R are provided in the Appendix. Using these definitions, the partition function Z can be expressed as a Grassmann tensor network [24],

$$Z = \text{gTr} \left[\prod_n \mathcal{T}_{\Psi_1(n) \Psi_2(n) \Psi_3(n) \Psi_4(n) \bar{\Psi}_4(n-4) \bar{\Psi}_3(n-3) \bar{\Psi}_2(n-2) \bar{\Psi}_1(n-1)} \right]. \tag{2.16}$$

Here, gTr denotes the Grassmann trace, i.e., the integration over the auxiliary Grassmann variables Ψ and $\bar{\Psi}$ in the sense of Eq. (2.7).

To evaluate Eq. (2.16), we have employed the Grassmann-anisotropic TRG method [13, 15] with the bond dimension D incorporating the multi-GPU parallelization technique proposed in Ref. [41].

3 Numerical results

Before presenting the results for the physical quantities, we check the convergence behavior of the thermodynamic potential $f(m, \mu, \lambda, D) = \ln Z(m, \mu, \lambda, D)/V$ by defining the quantity

$$\delta f(m, \mu, \lambda, D) = \left| \frac{\ln Z(m, \mu, \lambda, D) - \ln Z(m, \mu, \lambda, D=60)}{\ln Z(m, \mu, \lambda, D=60)} \right| \tag{3.1}$$

on $V = 1024^4$. Figure 1 shows the D dependence of δf at $(m, \lambda) = (1.0, 0)$ with the choices of $\mu = 1.08$ and 1.12 , the former of which resides in the Silver Blaze region and the latter in the region of the diquark condensation, as shown below. We observe good convergence behaviors for both cases: δf reaches $O(10^{-4})$ at $D = 55$. Hereafter, we present the results at $D = 55$ and omit the argument D in the functions of f and Z .

3.1 Chiral condensate and number density

We first show the results for the expectation values of the chiral condensate $\langle \bar{\chi} \chi \rangle$ and the quark number density $\langle n \rangle$ employing the numerical derivative of the thermodynamic

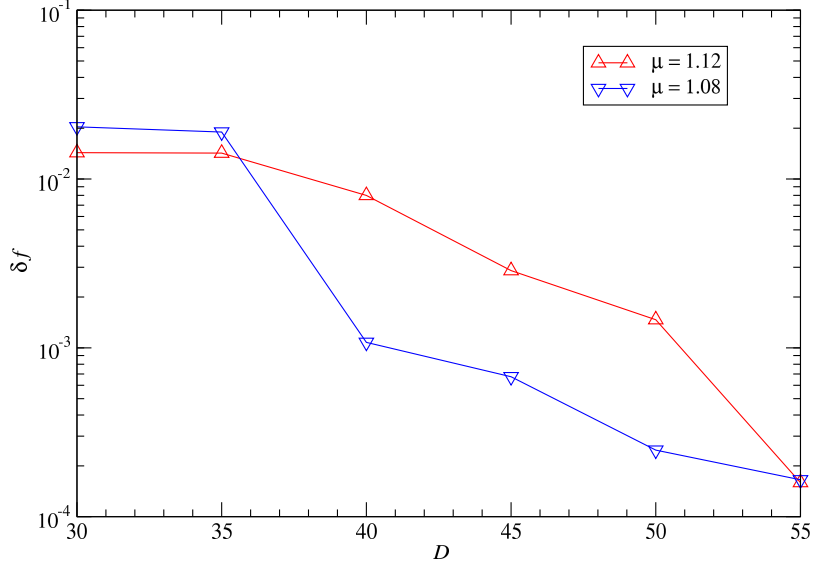


Figure 1: Convergence behaviors of thermodynamic potential as a function of D at $(m, \lambda) = (1.0, 0)$ on a 1024^4 . $\mu = 1.08$ and 1.12 cases are plotted.

potential:

$$\langle \bar{\chi} \chi \rangle = \frac{1}{V} \frac{\partial \ln Z(m, \mu, \lambda = 0)}{\partial m} \simeq \frac{1}{V} \frac{\ln Z(m + \Delta m, \mu, \lambda = 0) - \ln Z(m - \Delta m, \mu, \lambda = 0)}{2\Delta m}, \quad (3.2)$$

$$\begin{aligned} \langle n \rangle &= \frac{1}{V} \frac{\partial \ln Z(m, \mu, \lambda = 0)}{\partial \mu} \\ &\simeq \frac{1}{V} \frac{\ln Z(m, \mu + \Delta \mu, \lambda = 0) - \ln Z(m, \mu - \Delta \mu, \lambda = 0)}{2\Delta \mu} \end{aligned} \quad (3.3)$$

with $\Delta m = 0.02$ and $\Delta \mu = 0.02$.

Figure 2 plots $\langle \bar{\chi} \chi \rangle$ and $\langle n \rangle$, together with the diquark condensate $\langle \chi \chi \rangle$, as a function of μ at $m = 1.0$ on a 1024^4 lattice with the choice of $D = 55$. We find that the qualitative behaviors of $\langle \bar{\chi} \chi \rangle$ and $\langle n \rangle$ are similar to those for $m \neq 0$ given by the MF analysis in Ref. [4]: $\langle \bar{\chi} \chi \rangle$ stays constant up to $\mu = \mu_c^{\text{low}}$ and monotonically decreases up to the vanishing point of $\mu = \mu_c^{\text{up}}$, where $\mu_c^{\text{low}} \leq \mu \leq \mu_c^{\text{up}}$ is the region of $\langle \chi \chi \rangle \neq 0$; $\langle n \rangle/2$ starts to increase from zero at $\mu = \mu_c^{\text{low}}$ and saturates to $\langle n \rangle/2 = 1$ at $\mu \geq \mu_c^{\text{up}}$. Note that $\langle n \rangle > 2$ is not allowed due to the Pauli exclusion principle.

3.2 Diquark condensate

The diquark condensate is defined by

$$\langle \chi \chi \rangle = \frac{1}{V} \frac{\partial \ln Z(m, \mu, \lambda)}{\partial \lambda} \bigg|_{\lambda \rightarrow 0}. \quad (3.4)$$

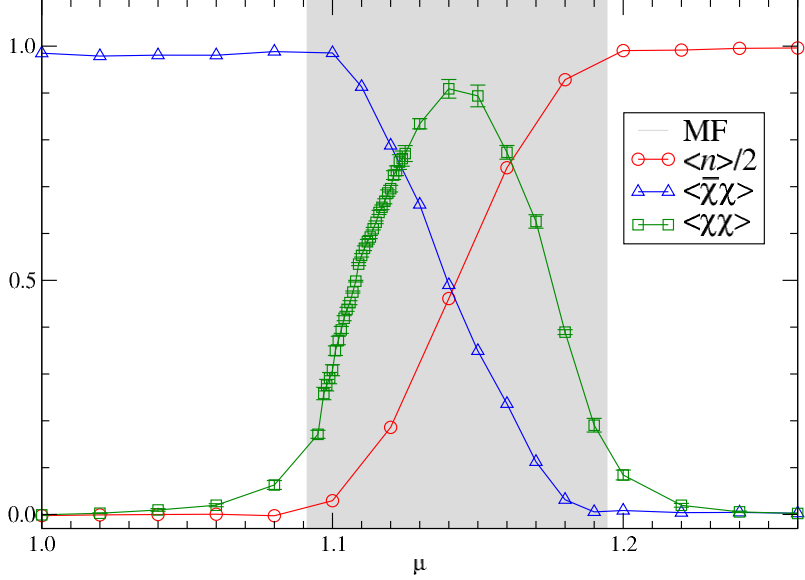


Figure 2: μ dependence of $\langle \bar{\chi}\chi \rangle$, $\langle \chi\chi \rangle$ and $\langle n \rangle/2$ at $(m, \lambda) = (1.0, 0)$ on a 1024^4 lattice with $D = 55$.

In order to avoid instabilities of the numerical derivative in terms of λ in the vicinity of $\lambda = 0$, we evaluate the diquark condensate by fitting $f(m, \mu, \lambda)$ with the following function:

$$f(m, \mu, \lambda) = b_1 \lambda^2 + b_2 |\lambda| + f(m, \mu, \lambda = 0), \quad (3.5)$$

where the coefficient b_2 gives the diquark condensate. The range of λ was chosen depending on μ : for $\mu = 1.095$, $\lambda \in [0, 0.030]$ with $\Delta\lambda = 0.002$, for $1.097 \leq \mu \leq 1.11$, $\lambda \in [0, 0.045]$ with $\Delta\lambda = 0.005$, and for other μ , $\lambda \in [0, 0.040]$ with $\Delta\lambda = 0.005$. We find that the μ dependence of the diquark condensate in Fig. 2 is qualitatively described by the MF analysis in Ref. [4]. The region of $\langle \chi\chi \rangle \neq 0$ shows rough consistency with the MF prediction, which is denoted by the gray band from $\mu_c^{\text{low}} = 1.0913$ to $\mu_c^{\text{up}} = 1.1944$.

Now let us determine the critical exponents β_m and δ . Figure 3 shows the μ dependence of $\langle \chi\chi \rangle$ with $D = 55$ near the critical point μ_c^{low} . A fit of $\langle \chi\chi \rangle$ in the region of $\mu \in [1.10, 1.12]$ assuming $\langle \chi\chi \rangle = A(\mu - \mu_c^{\text{low}})^{\beta_m}$ with A , μ_c^{low} and β_m the free parameters yields $A = 4.7(4)$, $\mu_c^{\text{low}} = 1.0950(7)$ and $\beta_m = 0.514(27)$. The value of the critical μ is close to the MF prediction of $\mu_c^{\text{low}} = 1.0913$ and β_m shows consistency with the MF prediction of $\beta_m = 0.5$. The lower limit of the fitting range is chosen to avoid the immediate vicinity of the critical point. Below $\mu = 1.10$ non-analytic behaviors of $f(m, \mu, \lambda)$ in terms of λ becomes manifest. The robustness of the fit results against the change of the upper limit of the fitting range is indicated by the fact that the data in the region of $1.12 < \mu \leq 1.13$ is on the fit curve. We also estimate another critical exponent δ from the λ dependence of the free energy at $\mu_c^{\text{low}} = 1.095$ plotted in Fig. 4. The solid curve denotes the fit results of the form $f(m, \mu, \lambda = 0) + b_0 \lambda^{1+1/\delta}$ choosing the fitting range of $\lambda \in [0, 0.03]$. The free parameters are determined as $b_0 = 1.51(6)$ and $\delta = 2.44(6)$. The value of δ is slightly smaller than the

MF prediction of $\delta = 3$. The discrepancy may be attributed to the difficulty in the precise determination of μ_c^{low} .

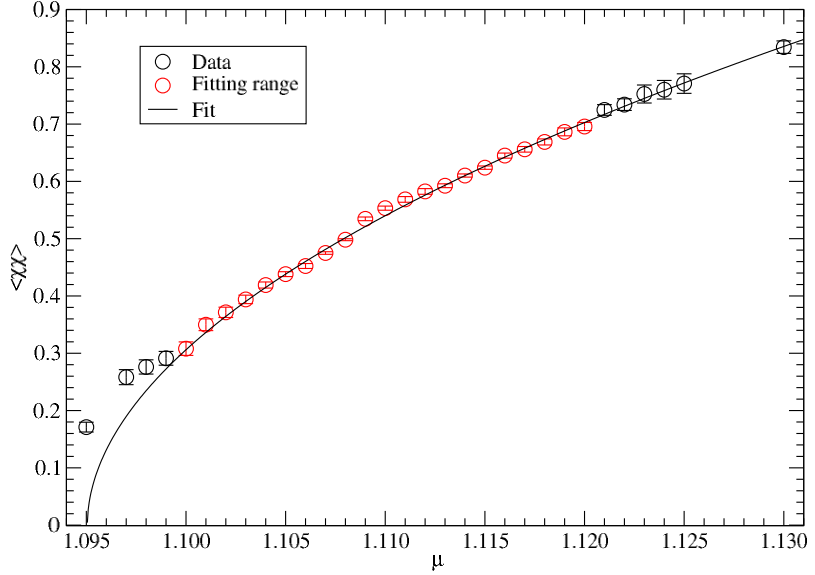


Figure 3: μ dependence of $\langle\chi\chi\rangle$ around μ_c^{low} at $(m, \lambda) = (1.0, 0)$ on a 1024^4 lattice with $D = 55$.

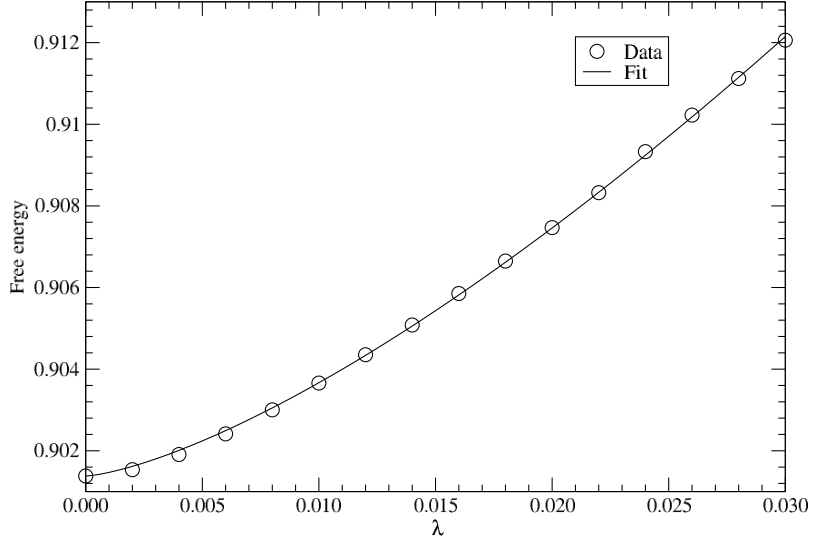


Figure 4: λ dependence of $\langle\chi\chi\rangle$ at $(m, \mu) = (1.0, 1.095)$ on a 1024^4 lattice with $D = 55$.

4 Summary and outlook

We have investigated the phase structure of the $(3+1)d$ finite density QC₂D at $m = 1.0$ on a 1024^4 lattice with $D = 55$. The volume is large enough to be regarded as the thermodynamic limit at zero temperature. The TRG results for the chiral and diquark

condensates and the number density show similar μ dependences to the previous MF results. The value of the critical exponents β_m is comparable to the MF prediction, while δ shows a slightly smaller value.

As a next step, it may be worthwhile to incorporate gauge fields at finite coupling. Another possible direction is an extension to the Wilson quark.

Acknowledgments

Numerical calculation for the present work was carried out using the computational resources of SQUID provided by Osaka University through the HPCI System Research Project (Project ID: hp250120). We also used Yukawa-21 at Yukawa Institute Computer Facility in Kyoto University and the supercomputer Pegasus under the Multidisciplinary Cooperative Research Program of Center for Computational Sciences, University of Tsukuba. Y.S. acknowledges support from the Graduate Program on Physics for the Universe (GP-PU), Tohoku University, and from JSPS KAKENHI (Grant-in-Aid for JSPS Fellows) Grant Number 25KJ0537. SA acknowledges the support from JSPS KAKENHI Grant Number JP23K13096, and the Top Runners in Strategy of Transborder Advanced Researches (TRiSTAR) program conducted as the Strategic Professional Development Program for Young Researchers by the MEXT. This work is supported in part by Grants-in-Aid for Scientific Research from the Ministry of Education, Culture, Sports, Science and Technology (MEXT) (Nos. 24H00214, 24H00940).

A Explicit form of F and R

We provide explicit form of the initial tensors. The Weingarten integration of link variables is expressed as follows:

$$\begin{aligned}
F_{i'^2 i'^1 j'^2 j'^1}^{a_\nu b_\nu c_\nu d_\nu} &= g(i'^2) g(i'^1) g(j'^2) g(j'^1) \int dU_\nu (U_\nu^{2a_\nu})^{i'^2} (U_\nu^{1b_\nu})^{i'^1} (U_\nu^{c_\nu 2^\dagger})^{j'^2} (U_\nu^{d_\nu 1^\dagger})^{j'^1} \\
&= \left[\delta_{0,i'^2} \delta_{0,i'^1} \delta_{0,j'^2} \delta_{0,j'^1} + \delta_{1,i'^2} \delta_{1,i'^1} \delta_{1,j'^2} \delta_{1,j'^1} \frac{1}{3} \left\{ \delta^{2,2} \delta^{a_\nu, c_\nu} \delta^{1,1} \delta^{b_\nu, d_\nu} - \frac{1}{2} \left(\delta^{2,2} \delta^{a_\nu, d_\nu} \delta^{1,1} \delta^{b_\nu, c_\nu} \right) \right\} \right. \\
&\quad + \frac{1}{2} \delta_{1,i'^2} \delta_{1,j'^2} \delta_{0,i'^1} \delta_{0,j'^1} (\delta^{a_\nu, c_\nu}) + \frac{1}{2} \delta_{0,i'^2} \delta_{0,j'^2} \delta_{1,i'^1} \delta_{1,j'^1} (\delta^{b_\nu, d_\nu}) \\
&\quad \left. + \delta_{1,i'^2} \delta_{1,i'^1} \delta_{0,j'^2} \delta_{0,j'^1} \frac{1}{2!} (\epsilon^{21} \epsilon^{a_\nu b_\nu}) + \delta_{0,i'^2} \delta_{0,i'^1} \delta_{1,j'^2} \delta_{1,j'^1} \frac{1}{2!} (\epsilon^{c_\nu d_\nu} \epsilon^{21}) \right] \\
&\quad \times g(i'^2) g(i'^1) g(j'^2) g(j'^1). \tag{A.1}
\end{aligned}$$

The difficulty in the Grassmann integration in Eq. (2.11) is that we cannot simply align staggered fields $\chi^1, \chi^2, \bar{\chi}^1, \bar{\chi}^2$ to a set order. To see this, we rewrite Eq. (2.11) in the following:

$$\mathcal{T} = \sum_{\{i,j\}} \int d\chi^1 d\bar{\chi}^1 d\chi^2 d\bar{\chi}^2 (1 - m\bar{\chi}^1 \chi^1 - m\bar{\chi}^2 \chi^2 + m^2 \bar{\chi}^1 \chi^1 \bar{\chi}^2 \chi^2) \left(\prod_\nu \sum_{a_\nu, b_\nu, c_\nu, d_\nu} \right) \left(\prod_\nu F_{i'^2 i'^1 j'^2 j'^1}^{a_\nu b_\nu c_\nu d_\nu} \right)$$

$$\begin{aligned}
& \times \left[\prod_{\nu} (\bar{\zeta}_{\nu}^2 \chi^{a_{\nu}})^{i_{\nu}^{12}} \right] \left[\prod_{\nu} (\bar{\zeta}_{\nu}^1 \chi^{b_{\nu}})^{i_{\nu}^{11}} \right] \left[\prod_{\nu} (\xi_{\nu}^1 \chi^1)^{j_{\nu}^1} \right] \left[\prod_{\nu} (\xi_{\nu}^2 \chi^2)^{j_{\nu}^2} \right] \\
& \times \left[\prod_{\nu} (\bar{\chi}^{c_{\nu}} \bar{\xi}_{\nu}^2)^{j_{\nu}^{12}} \right] \left[\prod_{\nu} (\bar{\chi}^{d_{\nu}} \bar{\xi}_{\nu}^1)^{j_{\nu}^{11}} \right] \left[\prod_{\nu} (\bar{\chi}^1 \zeta_{\nu}^1)^{i_{\nu}^1} \right] \left[\prod_{\nu} (\bar{\chi}^2 \zeta_{\nu}^2)^{i_{\nu}^2} \right]. \tag{A.2}
\end{aligned}$$

Examining Eq. (A.2), the ordering of the χ^1, χ^2 and $\bar{\chi}^1, \bar{\chi}^2$ depends on the choice of pairs of the primed variables i'_{ν}, j'_{ν} and the color indices $a_{\nu}, b_{\nu}, c_{\nu}, d_{\nu}$. Therefore, when performing the integration in the order $d\chi^1 d\bar{\chi}^1 d\chi^2 d\bar{\chi}^2$, a straightforward strategy is to absorb the corresponding sign factors into $F_{i_{\nu}^{12} i_{\nu}^{11} j_{\nu}^{12} j_{\nu}^{11}}^{a_{\nu} b_{\nu} c_{\nu} d_{\nu}}$. The final form is given by

$$\begin{aligned}
\tilde{F}_{i_{\nu}^{12} i_{\nu}^{11} j_{\nu}^{12} j_{\nu}^{11}}^{a_{\nu} b_{\nu} c_{\nu} d_{\nu}} = & \left[\delta_{0, i_{\nu}^{12}} \delta_{0, i_{\nu}^{11}} \delta_{0, j_{\nu}^{12}} \delta_{0, j_{\nu}^{11}} + \delta_{1, i_{\nu}^{12}} \delta_{1, i_{\nu}^{11}} \delta_{1, j_{\nu}^{12}} \delta_{1, j_{\nu}^{11}} \frac{1}{3} \left\{ \delta^{2,2} \delta^{a_{\nu}, c_{\nu}} \delta^{1,1} \delta^{b_{\nu}, d_{\nu}} + \frac{1}{2} \left(\delta^{2,2} \delta^{a_{\nu}, d_{\nu}} \delta^{1,1} \delta^{b_{\nu}, c_{\nu}} \right) \right\} \right. \\
& + \frac{1}{2} \delta_{1, i_{\nu}^{12}} \delta_{1, j_{\nu}^{12}} \delta_{0, i_{\nu}^{11}} \delta_{0, j_{\nu}^{11}} (\delta^{a_{\nu}, c_{\nu}}) + \frac{1}{2} \delta_{0, i_{\nu}^{12}} \delta_{0, j_{\nu}^{12}} \delta_{1, i_{\nu}^{11}} \delta_{1, j_{\nu}^{11}} (\delta^{b_{\nu}, d_{\nu}}) \\
& + \delta_{1, i_{\nu}^{12}} \delta_{1, i_{\nu}^{11}} \delta_{0, j_{\nu}^{12}} \delta_{0, j_{\nu}^{11}} \frac{1}{2!} \left(\epsilon^{21} |\epsilon^{a_{\nu} b_{\nu}}| \right) + \delta_{0, i_{\nu}^{12}} \delta_{0, i_{\nu}^{11}} \delta_{1, j_{\nu}^{12}} \delta_{1, j_{\nu}^{11}} \frac{1}{2!} \left(|\epsilon^{c_{\nu} d_{\nu}}| \epsilon^{21} \right) \left. \right] \\
& \times g(i_{\nu}^{12}) g(i_{\nu}^{11}) g(j_{\nu}^{12}) g(j_{\nu}^{11}).
\end{aligned}$$

By incorporating \tilde{F} instead of F into \mathcal{T} , we can effectively account for the complicated sign factors that arise in the integration.

After performing the integration, the auxiliary Grassmann variables ζ, ξ appear in the order

$$\left[\prod_{\nu} (\bar{\zeta}_{\nu}^2 \chi^{a_{\nu}})^{i_{\nu}^{12}} \right] \left[\prod_{\nu} (\bar{\zeta}_{\nu}^1 \chi^{b_{\nu}})^{i_{\nu}^{11}} \right] \left[\prod_{\nu} (\xi_{\nu}^1 \chi^1)^{j_{\nu}^1} \right] \left[\prod_{\nu} (\xi_{\nu}^2 \chi^2)^{j_{\nu}^2} \right] \tag{A.3}$$

$$\times \left[\prod_{\nu} (\bar{\chi}^{c_{\nu}} \bar{\xi}_{\nu}^2)^{j_{\nu}^{12}} \right] \left[\prod_{\nu} (\bar{\chi}^{d_{\nu}} \bar{\xi}_{\nu}^1)^{j_{\nu}^{11}} \right] \left[\prod_{\nu} (\bar{\chi}^1 \zeta_{\nu}^1)^{i_{\nu}^1} \right] \left[\prod_{\nu} (\bar{\chi}^2 \zeta_{\nu}^2)^{i_{\nu}^2} \right]. \tag{A.4}$$

To reorder them into the form of Eq. (2.11), we must include sign factors $(-1)^R$, where

$$\begin{aligned}
R_{(i_1^1, i_1^2, j_1^1, j_1^2)(i_2^1, i_2^2, j_2^1, j_2^2)(i_3^1, i_3^2, j_3^1, j_3^2)(i_4^1, i_4^2, j_4^1, j_4^2)(i_1'^1, i_1'^2, j_1'^1, j_1'^2)(i_2'^1, i_2'^2, j_2'^1, j_2'^2)(i_3'^1, i_3'^2, j_3'^1, j_3'^2)(i_4'^1, i_4'^2, j_4'^1, j_4'^2)} = & i_1^1 \left(\sum_{\nu=1}^4 j_{\nu}^{11} + \sum_{\nu=1}^4 j_{\nu}^{12} + \sum_{\nu=1}^4 j_{\nu}^{21} + \sum_{\nu=1}^4 j_{\nu}^{22} + \sum_{\nu=1}^4 i_{\nu}^{11} + \sum_{\nu=1}^4 i_{\nu}^{12} \right) \\
& + i_1^2 \left(\sum_{\nu=2}^4 i_{\nu}^1 + \sum_{\nu=1}^4 j_{\nu}^{11} + \sum_{\nu=1}^4 j_{\nu}^{12} + \sum_{\nu=1}^4 j_{\nu}^{21} + \sum_{\nu=1}^4 j_{\nu}^{22} + \sum_{\nu=1}^4 i_{\nu}^{11} + \sum_{\nu=1}^4 i_{\nu}^{12} \right) \\
& + j_1^1 \left(\sum_{\nu=1}^4 i_{\nu}^{11} + \sum_{\nu=1}^4 i_{\nu}^{12} \right) \\
& + j_1^2 \left(\sum_{\nu=2}^4 j_{\nu}^1 + \sum_{\nu=1}^4 i_{\nu}^{11} + \sum_{\nu=1}^4 i_{\nu}^{12} \right) + i_2^1 \left(\sum_{\nu=1}^4 j_{\nu}^{11} + \sum_{\nu=1}^4 j_{\nu}^{12} + \sum_{\nu=2}^4 j_{\nu}^{21} + \sum_{\nu=2}^4 j_{\nu}^{22} + \sum_{\nu=1}^4 i_{\nu}^{11} + \sum_{\nu=1}^4 i_{\nu}^{12} \right) \\
& + i_2^2 \left(\sum_{\nu=3}^4 i_{\nu}^1 + \sum_{\nu=1}^4 j_{\nu}^{11} + \sum_{\nu=1}^4 j_{\nu}^{12} + \sum_{\nu=2}^4 j_{\nu}^{21} + \sum_{\nu=2}^4 j_{\nu}^{22} + \sum_{\nu=1}^4 i_{\nu}^{11} + \sum_{\nu=1}^4 i_{\nu}^{12} \right)
\end{aligned}$$

$$\begin{aligned}
& + j_2^1 \left(\sum_{\nu=1}^4 i_\nu'^1 + \sum_{\nu=1}^4 i_\nu'^2 \right) + j_2^2 \left(\sum_{\nu=3}^4 j_\nu^1 + \sum_{\nu=1}^4 i_\nu'^1 + \sum_{\nu=1}^4 i_\nu'^2 \right) \\
& + i_3^1 \left(\sum_{\nu=1}^4 j_\nu'^1 + \sum_{\nu=1}^4 j_\nu'^2 + \sum_{\nu=3}^4 j_\nu^2 + \sum_{\nu=3}^4 j_\nu^1 + \sum_{\nu=1}^4 i_\nu'^1 + \sum_{\nu=1}^4 i_\nu'^2 \right) \\
& + i_3^2 \left(i_4^1 + \sum_{\nu=1}^4 j_\nu'^1 + \sum_{\nu=1}^4 j_\nu'^2 + \sum_{\nu=3}^4 j_\nu^2 + \sum_{\nu=3}^4 j_\nu^1 + \sum_{\nu=1}^4 i_\nu'^1 + \sum_{\nu=1}^4 i_\nu'^2 \right) \\
& + j_3^1 \left(\sum_{\nu=1}^4 i_\nu'^1 + \sum_{\nu=1}^4 i_\nu'^2 \right) + j_3^2 \left(j_4^1 + \sum_{\nu=1}^4 i_\nu'^1 + \sum_{\nu=1}^4 i_\nu'^2 \right) \\
& + i_4^1 \left(\sum_{\nu=1}^4 j_\nu'^1 + \sum_{\nu=1}^4 j_\nu'^2 + j_4^2 + j_4^1 + \sum_{\nu=1}^4 i_\nu'^1 + \sum_{\nu=1}^4 i_\nu'^2 \right) \\
& + i_4^2 \left(\sum_{\nu=1}^4 j_\nu'^1 + \sum_{\nu=1}^4 j_\nu'^2 + j_4^2 + j_4^1 + \sum_{\nu=1}^4 i_\nu'^1 + \sum_{\nu=1}^4 i_\nu'^2 \right) \\
& + j_4^1 \left(\sum_{\nu=1}^4 i_\nu'^1 + \sum_{\nu=1}^4 i_\nu'^2 \right) + j_4^2 \left(\sum_{\nu=1}^4 i_\nu'^1 + \sum_{\nu=1}^4 i_\nu'^2 \right) \\
& + j_4'^2 \left(\sum_{\nu=1}^3 j_\nu'^2 + \sum_{\nu=1}^4 i_\nu'^1 + \sum_{\nu=1}^4 i_\nu'^2 \right) + j_4'^1 \left(\sum_{\nu=1}^3 j_\nu'^1 + \sum_{\nu=1}^3 j_\nu'^2 + \sum_{\nu=1}^4 i_\nu'^1 + \sum_{\nu=1}^4 i_\nu'^2 \right) \\
& + i_4'^2 \left(\sum_{\nu=1}^3 i_\nu'^2 \right) + i_4'^1 \left(\sum_{\nu=1}^3 i_\nu'^1 + \sum_{\nu=1}^3 i_\nu'^2 \right) \\
& + j_3'^2 \left(\sum_{\nu=1}^2 j_\nu'^2 + \sum_{\nu=1}^3 i_\nu'^1 + \sum_{\nu=1}^3 i_\nu'^2 \right) + j_3'^1 \left(\sum_{\nu=1}^2 j_\nu'^1 + \sum_{\nu=1}^2 j_\nu'^2 + \sum_{\nu=1}^3 i_\nu'^1 + \sum_{\nu=1}^3 i_\nu'^2 \right) + i_3'^2 \left(\sum_{\nu=1}^2 i_\nu'^2 \right) \\
& + i_3'^1 \left(\sum_{\nu=1}^2 i_\nu'^1 + \sum_{\nu=1}^2 i_\nu'^2 \right) \\
& + j_2'^2 \left(j_1'^2 + \sum_{\nu=1}^2 i_\nu'^1 + \sum_{\nu=1}^2 i_\nu'^2 \right) \\
& + j_2'^1 \left(j_1'^1 + j_1'^2 + \sum_{\nu=1}^2 i_\nu'^1 + \sum_{\nu=1}^2 i_\nu'^2 \right) + i_2'^2 i_1'^2 + i_2'^1 (i_1'^1 + i_1'^2) \\
& + j_1'^2 (i_1'^1 + i_1'^2) + j_1'^1 (i_1'^1 + i_1'^2).
\end{aligned}$$

Finally, we briefly comment on the numerical strategy for constructing the initial tensor in Eq. (2.15). Since the size of T is 16^8 , it is impractical to implement a naive for-loop over all indices. However, careful inspection of the Kronecker delta constraints arising from the fermion and link variable integrations in Eq. (2.15) shows that they restrict nonzero contributions to only a small subset of entries, yielding a highly sparse and low-rank structure. Therefore, we performed for-loops only over the indices allowed by the Kronecker delta constraints and constructed T in the form of a sparse matrix. To generate the fundamental tensors required in the ATRG method, we applied truncated SVD to T

using Arpack [42].

References

- [1] E. Dagotto, F. Karsch and A. Moreo, *The Strong Coupling Limit of $SU(2)$ QCD at Finite Baryon Density*, *Phys. Lett. B* **169** (1986) 421–427.
- [2] E. Dagotto, A. Moreo and U. Wolff, *Lattice $SU(N)$ QCD at Finite Temperature and Density in the Strong Coupling Limit*, *Phys. Lett. B* **186** (1987) 395–400.
- [3] J. U. Klatke and K. H. Mutter, *Strong Coupling QCD With $SU(2)$ Gauge Fields at Finite Baryon Number Density*, *Nucl. Phys. B* **342** (1990) 764–780.
- [4] Y. Nishida, K. Fukushima and T. Hatsuda, *Thermodynamics of strong coupling two color QCD with chiral and diquark condensates*, *Phys. Rept.* **398** (2004) 281–300, [[hep-ph/0306066](#)].
- [5] Y. Nishida, *Phase structures of strong coupling lattice QCD with finite baryon and isospin density*, *Phys. Rev. D* **69** (2004) 094501, [[hep-ph/0312371](#)].
- [6] M. Levin and C. P. Nave, *Tensor renormalization group approach to two-dimensional classical lattice models*, *Phys. Rev. Lett.* **99** (2007) 120601, [[cond-mat/0611687](#)].
- [7] Z. Y. Xie, J. Chen, M. P. Qin, J. W. Zhu, L. P. Yang and T. Xiang, *Coarse-graining renormalization by higher-order singular value decomposition*, *Phys. Rev. B* **86** (Jul, 2012) 045139, [[1201.1144](#)].
- [8] Y. Shimizu and Y. Kuramashi, *Grassmann tensor renormalization group approach to one-flavor lattice Schwinger model*, *Phys. Rev. D* **90** (2014) 014508, [[1403.0642](#)].
- [9] G. Evenbly and G. Vidal, *Tensor network renormalization*, *Phys. Rev. Lett.* **115** (Oct, 2015) 180405.
- [10] R. Sakai, S. Takeda and Y. Yoshimura, *Higher order tensor renormalization group for relativistic fermion systems*, *PTEP* **2017** (2017) 063B07, [[1705.07764](#)].
- [11] S. Yang, Z.-C. Gu and X.-G. Wen, *Loop optimization for tensor network renormalization*, *Phys. Rev. Lett.* **118** (Mar, 2017) 110504.
- [12] M. Hauru, C. Delcamp and S. Mizera, *Renormalization of tensor networks using graph independent local truncations*, *Phys. Rev. B* **97** (2018) 045111, [[1709.07460](#)].
- [13] D. Adachi, T. Okubo and S. Todo, *Anisotropic Tensor Renormalization Group*, *Phys. Rev. B* **102** (2020) 054432, [[1906.02007](#)].
- [14] D. Kadoh and K. Nakayama, *Renormalization group on a triad network*, [1912.02414](#).
- [15] S. Akiyama, Y. Kuramashi, T. Yamashita and Y. Yoshimura, *Restoration of chiral symmetry in cold and dense Nambu–Jona-Lasinio model with tensor renormalization group*, *JHEP* **01** (2021) 121, [[2009.11583](#)].
- [16] D. Adachi, T. Okubo and S. Todo, *Bond-weighted tensor renormalization group*, *Phys. Rev. B* **105** (Feb, 2022) L060402, [[2011.01679](#)].
- [17] S. Akiyama, *Bond-weighting method for the Grassmann tensor renormalization group*, *JHEP* **11** (2022) 030, [[2208.03227](#)].

- [18] Y. Shimizu and Y. Kuramashi, *Critical behavior of the lattice Schwinger model with a topological term at $\theta = \pi$ using the Grassmann tensor renormalization group*, *Phys. Rev. D* **90** (2014) 074503, [[1408.0897](#)].
- [19] H. Kawauchi and S. Takeda, *Tensor renormalization group analysis of $CP(N-1)$ model*, *Phys. Rev. D* **93** (2016) 114503, [[1603.09455](#)].
- [20] H. Kawauchi and S. Takeda, *Loop-TNR analysis of $CP(1)$ model with theta term*, *EPJ Web Conf.* **175** (2018) 11015, [[1710.09804](#)].
- [21] L.-P. Yang, Y. Liu, H. Zou, Z. Xie and Y. Meurice, *Fine structure of the entanglement entropy in the $O(2)$ model*, *Phys. Rev. E* **93** (2016) 012138, [[1507.01471](#)].
- [22] Y. Shimizu and Y. Kuramashi, *Berezinskii-Kosterlitz-Thouless transition in lattice Schwinger model with one flavor of Wilson fermion*, *Phys. Rev. D* **97** (2018) 034502, [[1712.07808](#)].
- [23] S. Takeda and Y. Yoshimura, *Grassmann tensor renormalization group for the one-flavor lattice Gross-Neveu model with finite chemical potential*, *PTEP* **2015** (2015) 043B01, [[1412.7855](#)].
- [24] D. Kadoh, Y. Kuramashi, Y. Nakamura, R. Sakai, S. Takeda and Y. Yoshimura, *Tensor network formulation for two-dimensional lattice $\mathcal{N} = 1$ Wess-Zumino model*, *JHEP* **03** (2018) 141, [[1801.04183](#)].
- [25] D. Kadoh, Y. Kuramashi, Y. Nakamura, R. Sakai, S. Takeda and Y. Yoshimura, *Investigation of complex ϕ^4 theory at finite density in two dimensions using TRG*, *JHEP* **02** (2020) 161, [[1912.13092](#)].
- [26] S. Takeda, *Tensor network approach to real-time path integral*, *PoS LATTICE2019* (2019) 033, [[1908.00126](#)].
- [27] Y. Kuramashi and Y. Yoshimura, *Tensor renormalization group study of two-dimensional $U(1)$ lattice gauge theory with a θ term*, *JHEP* **04** (2020) 089, [[1911.06480](#)].
- [28] S. Akiyama, D. Kadoh, Y. Kuramashi, T. Yamashita and Y. Yoshimura, *Tensor renormalization group approach to four-dimensional complex ϕ^4 theory at finite density*, *JHEP* **09** (2020) 177, [[2005.04645](#)].
- [29] K. Nakayama, L. Funcke, K. Jansen, Y.-J. Kao and S. Kühn, *Phase structure of the $CP(1)$ model in the presence of a topological θ -term*, *Phys. Rev. D* **105** (2022) 054507, [[2107.14220](#)].
- [30] J. Bloch, R. G. Jha, R. Lohmayer and M. Meister, *Tensor renormalization group study of the three-dimensional $O(2)$ model*, *Phys. Rev. D* **104** (2021) 094517, [[2105.08066](#)].
- [31] J. Bloch and R. Lohmayer, *Grassmann higher-order tensor renormalization group approach for two-dimensional strong-coupling QCD*, *Nucl. Phys. B* **986** (2023) 116032, [[2206.00545](#)].
- [32] S. Akiyama and Y. Kuramashi, *Critical endpoint of (3+1)-dimensional finite density \mathbb{Z}_3 gauge-Higgs model with tensor renormalization group*, *JHEP* **10** (2023) 077, [[2304.07934](#)].
- [33] S. Akiyama and Y. Kuramashi, *Tensor renormalization group study of (1 + 1)-dimensional $U(1)$ gauge-Higgs model at $\theta = \pi$ with Lüscher's admissibility condition*, *JHEP* **09** (2024) 086, [[2407.10409](#)].
- [34] X. Luo and Y. Kuramashi, *Tensor renormalization group approach to (1+1)-dimensional $SU(2)$ principal chiral model at finite density*, *Phys. Rev. D* **107** (2023) 094509, [[2208.13991](#)].

- [35] M. Hite and Y. Meurice, *Quantum real-time evolution using tensor renormalization group methods*, *Phys. Rev. D* **111** (2025) 034502, [[2411.05301](#)].
- [36] X. Luo and Y. Kuramashi, *Quantum phase transition of (1+1)-dimensional $O(3)$ nonlinear sigma model at finite density with tensor renormalization group*, *JHEP* **11** (2024) 144, [[2406.08865](#)].
- [37] X. Luo and Y. Kuramashi, *Critical endpoints of three-dimensional finite density $SU(3)$ spin model with tensor renormalization group*, *JHEP* **07** (2025) 036, [[2503.05144](#)].
- [38] K. H. Pai, S. Akiyama and S. Todo, *Grassmann tensor renormalization group approach to (1+1)-dimensional two-color lattice QCD at finite density*, *JHEP* **03** (2025) 027, [[2410.09485](#)].
- [39] S. Akiyama and D. Kadoh, *More about the Grassmann tensor renormalization group*, *JHEP* **10** (2021) 188, [[2005.07570](#)].
- [40] D. Weingarten, *Asymptotic Behavior of Group Integrals in the Limit of Infinite Rank*, *J. Math. Phys.* **19** (1978) 999.
- [41] Y. Sugimoto and S. Sasaki, *Triad Representation for the Anisotropic Tensor Renormalization Group in Four Dimensions*, [2507.21909](#).
- [42] R. B. Lehoucq, D. C. Sorensen and C. Yang, *ARPACK Users' Guide*. Society for Industrial and Applied Mathematics, 1998, [10.1137/1.9780898719628](#).